Contents lists available at ScienceDirect

European Polymer Journal

Macromolecular Nanotechnology

Comparative studies for the effect of intercalating agent on the physical properties of epoxy resin-clay based nanocomposite materials

Chung-Feng Dai, Pei-Ru Li, Jui-Ming Yeh *

*Department of Chemistry, Center for Nanotechnology at CYCU and R&D Center for Membrane Technology,
Chung-Yuan Christian University, Chung Li 32023, Taiwan, ROC*

A R T I C L E   I N F O

A B S T R A C T

In this study, a series of comparative studies for the effect of intercalating agent on the physical properties of the epoxy resin-clay based nanocomposite materials were performed. First, the quaternary alkylphosphonium and alkylammonium salt were both used as the intercalating agents separately for the preparation of organophilic clay through the cationic exchange reactions with Na^+-montmorillonite clay. Subsequently, the organophilic clay was blent into the epoxy resin through *in-situ* thermal ring-opening polymerizations to prepare a series of polymer-clay nanocomposite (PCN) materials. The as-synthesized PCN materials were subsequently characterized by Fourier-Transformation infrared (FTIR) spectroscopy, wide-angle powder X-ray diffraction (WXRD), and transmission electron microscopy (TEM).

It should be noted that the quaternary alkylphosphonium salt (Φ_3P^+-C_{12})-modified clay was found to show better dispersion capability than that of quaternary alkylammonium salt (Me_3N^+-C_{16})-modified clay existed in the polymer matrix based on the studies of WXRD and TEM. The better dispersion of (Φ_3P^+-C_{12})-modified clay in epoxy resin was found to lead more effectively enhanced physical property such as corrosion protection, gas barrier, mechanical strength, thermal stability, and flame retardant properties of polymers than that of (Me_3N^+-C_{16})-modified clay, in the form of coating and membrane, based on the measurements of a series of electrochemical corrosion parameters, gas permeability analysis (GPA), dynamic mechanical analysis (DMA), differential scanning calorimetry (DSC), thermogravimetric analysis (TGA), and limiting oxygen index (LOI), respectively. Effect of material composition on the physical properties of as-prepared materials was also investigated.

Crown Copyright © 2008 Published by Elsevier Ltd. All rights reserved.

1. Introduction

Nanocomposite materials consisted of organic polymeric matrix and inorganic nano-layered clay platelets have lately evoked a great deal of academic and industrial research activities due to their uniqueness of combining the organic and inorganic characteristics at the molecular level, leading to the formation of nanocomposite materials with effectively enhanced physical properties such as thermal properties (e.g., thermal stability [1], flame retardant [2], thermal conductivity [3]), mechanical properties (e.g., mechanical strength [4], hardness [5], abrasion resistance [6]), electro-rheological properties [7], permeability properties (e.g., gas barrier [8], pervaporation [9]) and corrosion protection properties [10] of polymers.

Currently, Na^+-montmorillonite (Na^+-MMT) clay is widely used in the preparation of polymer nanocomposite materials because its lamellar elements exhibit high in-plane strength, stiffness, and high aspect ratio. Typically, the chemical structures of MMT consist of two fused silica tetrahedral sheets sandwiching an edge-shared octahedral sheet of either magnesium or aluminum hydroxide. The Na^+ and Ca^{2+} residing in the interlayer regions usually

* Corresponding author. Tel.: +886 3 2653340; fax: +886 3 2653399.
  E-mail address: juiming@cycu.edu.tw (J.-M. Yeh).

can be replaced by organic cations such as alkylammonium ions by a cationic-exchange reaction to render the hydrophilic-layered silicate organophilic. The organophilically charged clay layers exchanged by cationic surfactants playing an important role for the intercalation.

In the past decades, thermosetting polymers such as epoxy resin, polyimide or phenolic resins attracted many chemists, physicists, and material scientists devoting efforts to study their nanocomposites. Among these thermosets, epoxy resins evoked intensive studies much in the preparation of nanocomposite materials lately due to their high tensile strength, and modulus, good adhesive properties, good chemical, and corrosion resistance, low shrinkage in cure, and excellent dimensional stability. Up to date, many published literatures in terms of the investigations of epoxy resin-clay nanocomposite materials have been reported and concentrated mainly on the exploration of mechanical and thermal properties based on the comparative studies between nanocomposites containing raw Na^+-MMT and organophilic clay [11]. However, effect of different intercalation agent on physical properties of nanocomposite materials has seldom been mentioned.

Therefore, in this study, we present a series of comparative studies for the effect of intercalating agent on physical properties of epoxy resin-clay based nanocomposite materials. The as-synthesized nanopcomposite materials were subsequently characterized by FTIR spectroscopy, WXRD, and TEM.

Effect of intercalation agent used on the physical properties of nanocomposite materials (e.g., corrosion protection, gas barrier, mechanical strength, thermal stability, and flame retardant properties) in the form of coating and membrane, was evaluated a series of based on the measurements of electrochemical corrosion parameters, GPA, DMA, DSC, TGA, and LOI, respectively. Furthermore, effect of material composition on the physical properties was also investigated.

2. Experimental

2.1 Materials and instrumentations

Triphenylolmethane triglycidyl ether (TGTPM) (Aldrich), N,N-dimethylacetamide (DMAc) (99%; Riedel-deHaën). Hydrochloric acid (37%; Riedel-deHaën) is applied to prepare the 1.0 M HCl aqueous solution, and potassium bromide (KBr) (Riedel-deHaën) is used as received without further purification. The used Na^+-montmorillonite clay (PK 802) consisted of a unit cell formula $Ca_{0.084}$-$Na_{0.143}(Al_{1.69}Mg_{0.31})Si_4O_{10}(OH)_2 \cdot 2H_2O$, which CEC (cation exchange capacity) value of 115 mEq/100 g is purchased from Pai-Kong Ceramic Company, Taiwan. Trimethylolpropane tris [poly (propylene glycol), amine terminated] ether (T-403) (Aldrich) was used as hardener. Dodecyl triphenylphosphonium bromide (98%; Aldrich), hexadecyltirmethyl-ammonium bromide (99%; Sigma), were both employed as intercalating agents.

Fourier Transform Infrared spectra were recorded from pressed KBr pellets coated with PCN materials and obtained at a resolution of 4.0 cm^{-1} with a FTIR (BIO-RAD FTS-7) at room temperature ranging from 4000 to 400 cm^{-1}. WXRD study of the samples was performed on a Panalytical X′Pert Pro X-ray diffractometer with copper target and Ni filter at a scanning rate of 2°/min. The samples for TEM study were first prepared by putting the membrane of PCN materials into low-viscosity embedding media capsules with four ingredients (ERL4204 5.0 g, DER736 3.0 g, NSA 13.0 g, and DMAE 0.15 g) and by curing the media at 80 °C for 12 h in vacuum oven. Then the cured capsules containing PCN materials were microtomed with Leica Ultracut Uct into 90-nm-thick slices. Subsequently, one layer of carbon about 10 nm thick was deposited on these slices on mesh 100 copper nets for TEM observations on a JEOL-200FX with an acceleration voltage of 120 kV. Electrochemical corrosion measurements were performed on a VoltaLab Model 21 and VoltaLab Model 40 Potentiostat/Galvanostat in a standard corrosion cell equipped with two graphite rod counter-electrodes and a saturated calomel electrode (SCE) as well as a working electrode. A Yanagimoto gas permeability analyzer (model GTR-10) is employed to perform the permeation experiment of oxygen and nitrogen gas. The permeation of water vapor was performed using the apparatus employed in our previous published literatures [10]. TGA and DSC were employed to record the thermal stability of specimens. TGA scans were performed on a DuPont TA Q50 thermal analysis system in N_2 and air flow. The scan rate was 10 °C/min, and temperature range was from 30 °C to 900 °C. DSC was performed on a DuPont TA Q10 differential scanning calorimeter at a heating or cooling rate of 10 °C/min in nitrogen atmosphere. The temperature range was from 30 °C to 200 °C. The glass transition temperature (T_g) of the PCN materials were recorded based on the second scanning. The mechanical behaviors of all PCN materials under uni-axial tension (1 N/min) were measured on a DMA which were performed from 30 °C to 200 °C with a DuPont TA Q800 analyzer at a heating rate of 3 °C/min and at a frequency of 1 Hz. LOI values were measured on a United States Testing 8100 flame meter by a modified method that was previously investigated in the literature [12–14]. The percentage in the O_2/N_2 mixture deemed sufficient to sustain the flame was taken as the LOI.

2.2. Preparation of organophilic clay

The organophilic clay was prepared by a cationic exchange method, which is a reaction between the sodium cations of MMT clay and both intercalation agents of dodecyltriphenyl-phosphonium bromide (Φ_3P^+-C_{12}), and hexadecyltirmethyl-ammonium bromide (Me_3N^+-C_{16}) [10]. Typically, 5 g of MMT clay with a CEC value of 115 mEq/100 g was stirred in 500 mL of distilled water (beaker A) at room temperature overnight. The quantity of intercalation agent used was calculated from the following equation:

$$\frac{CEC \text{ of clay(mEq)} \times clay(g) \times 1.5}{100(g)}$$
$$= \frac{Intercalating \text{ agent}(g) \times 1000}{Mw \text{ of intercalating agent}(g/mol)} \quad (1)$$

where 115 mEq/100 g represented the CEC value per 100 g of MMT clay, and 1.5 (>1) indicated the excess amount of intercalating agent used. As calculated from above, a separate solution containing 3.438 g (7 mmol) of Φ_3P^+-C_{12} in another 50 mL of distilled water (beaker B) was under magnetically stirring, follows by adding 1.0 M HCl aqueous solution to adjust the pH value to about 3–4. After stirring for 3 h, the solution of beaker B was added at a rate of approximately 10 mL/min with vigorous stirring to the MMT suspension (beaker A). The mixture was stirred overnight at room temperature. The organophilic clay was recovered by ultracentrifugating (9000 rpm, 30 min) and then decanting the clear solution. Purification of products is performed by washing with 500 mL of distilled water for 0.5–1 h and then ultracentrifugating (9000 rpm, 30 min) samples repeated for five times to remove any excess ammonium ions. Upon drying under dynamic vacuum for 48 h at 40 °C, the organophilic clay was obtained. On the other hand, the preparation of quaternary ammonium salt-modified organophilic clay was followed similar preparative steps to that of quaternary phosphonium salt-modified clay [10].

2.3. In-situ synthesis of epoxy resin-clay nanocomposite materials

The typical procedure to prepare the epoxy resin-clay nanocomposites with two systems containing two different intercalating agents was given as follows: For example, 1 g of TGTPM was dissolved in 12 g of DMAc under stirring for 6 h. The as-prepared organophilic MMT clay modified with Φ_3P^+-C_{12} and Me_3N^+-C_{16} as mentioned above in various feeding composition of 0, 1, 3, 5, and 7 wt% was introduced, subsequently, 0.54 g of T-403 functioned as curing agent was added with further stirring for 12 h at room temperature. The resultant mixture was degassed and drop-wisely cast onto a clean Teflon mould followed by curing at 140 °C for 6 h. The cured epoxy membrane was obtained with a thickness of ca. ∼0.175 mm.

2.4. Preparation of coating and electrochemical measurements

As a representative procedure to prepare sample-coated coupons for electrochemical measurements, fresh-solutions of epoxy or epoxy resin-clay nanocomposite materials in DMAc were cast dropwisely onto the cold-rolled steel (CRS) with dimensions of 1×1 cm^2 and the coating treated by drying in air for 6 h at 140 °C to give an average thickness of ca. ∼0.36 mm, measured by a digimatic micrometer (Mitutoyo). The coated and uncoated coupons were then mounted to the working electrode so that only the so that only the coated side of the coupon was in direct contact with the electrolyte. The edges of the coupons were sealed with super fast epoxy cement (trade name SPAR$^®$). All of the corrosion potential, polarization resistance, and corrosion current were performed on a VoltaLab model 21 Potentiostat/Galvanostat in a standard corrosion test cell equipped with a graphite rod (diameter is 6.15 mm) counter-electrodes, a saturated calomel reference electrode (SCE), and a working electrode, then which experimental data were repeated at least five times. The

electrolyte was an aqueous solution containing 5 wt% of NaCl solution. Open circuit potential (OCP) at the equilibrium state of the system was recorded as the corrosion potential [E_{corr} (in V) vs. SCE]. Polarization resistance (R_p in Ω/cm^2) was measured by sweeping the applied potential from 20 mV below to 20 mV above the E_{corr} at a scan rate of 500 mV/min and by recording the corresponding current change. R_p values were obtained from the slope of the potential current plot. Tafel plots were obtained by scanning potential from 250 mV below to 250 mV above the E_{corr} at a scant rate of 500 mV/min. Corrosion current (I_{corr}) was determined by superimposing the straight line along the linear portion of the cathodic or anodic curve and extrapolating it through E_{corr}. The corrosion rate [R_{corr} in milli-inches per year (MPY)] was calculated from the following equation [10]:

$$R_{corr}(MPY) = [0.13 \times I_{corr} \times (E.W.)]/[A \times d] \qquad (2)$$

where E.W. is the equivalent weight (in g/eq.), A is the area (in cm^2), and d is the density (in g/cm^3).

On the other hand, impedance spectroscopy studies were also employed on a VoltaLab model 40 Potentiostat/Galvanostat, those were carried out in the frequency range of 100 kHz to 100 MHz. The working electrode was first maintained in the test environment for 30 min to reach an equilibrium state before the impedance operated. This condition serves to put the electrode in a reproducible initial state and to confirm that no blistering occurred during the conditioning period. All experiments were detected at room temperature of 27 ± 1 °C, and all data are replicated at least five times to confirm reproducibility and statistical significance.

2.5. Gas and water-vapor barrier property measurements

The sample-coated on the clear Teflon substrate was cured at 140 °C for 6 h. The films were lifted from Teflon plant to get membranes with thickness of ca. ∼0.17 mm, measured by digimatic micrometer (Mitutoyo).

Oxygen permeability of membrane was determined by using the Yanco GTR-10 gas permeability analyzer. Gas permeability was calculated by:

$$P = \ell/(p_1 - p_2) \times \frac{q/t}{A} \qquad (3)$$

where P was the gas permeability [cm^3(STP)-cm/cm^2-s-cmHg], q/t was the volumetric flow rate of gas permeate [cm^3(STP)/s], ℓ was the membrane thickness [cm], A was the effective membrane area [cm^2], and p_1, p_2 were the pressure (cmHg) on the high-pressure and low-pressure sides of the membrane, respectively. The rate of transmission of O_2 permeability was obtained by gas chromatography, from which the air permeability was calculated. On the other hand, the experiment of water-vapor permeation measurements was performed by using the same apparatus as pervaporation, except that the feed solution was not in contact with the membrane. It was performed by our previous published papers [10] wherein the feed solution vaporized first and subsequently permeated through the membrane with an effective area of ∼10.2 cm^2. The permeation rate was determined by measuring the weight of permeate.

2.6. Flame retardant performance measurements

The relative flammability of the molded epoxy resin-clay nanocomposite cured specimen was determined by an LOI tester (United States Testing 8100). According to below equation:

$$LOI = \frac{\text{vol. of } O_2}{\text{vol. of } O_2 + \text{vol. of } N_2} \times 100 \qquad (4)$$

The limiting oxygen index was the minimum concentration of oxygen determined in a flowing mixture of oxygen and nitrogen that will just support the flaming combustion of materials. The free-standing film samples (140 mm × 50 mm × 1 mm sheets) were placed in a glassy cylinder and situated in the middle of the chimney. The flame was applied from the top of the chimney till ignited 8 cm for 3 min, according to the standard "oxygen index" test ASTM D-2863. Each datum was obtained from three samples as an average value [15,16].

3. Results and discussion

In this work, one tri-functional epoxy as well as one tri-functional amine monomers for the formation of epoxy resin matrix and two different types of intercalation agents for the modification of Na+-MMT clay was used and their chemical structures were shown in Fig. 1. The two cationic surfactants were used for performing a series of comparative studies for the effect of intercalation agent on the physical properties of as-prepared materials. To prepare the polymer-clay nanocomposite materials, the intercalation agents (i.e., quaternary alkylphosphonium and alkylammonium salt) were first performing the cationic exchange reactions with the sodium ions existed in the intragallery region of Na+-MMT clay to give organophilic clay. Subsequently, the as-prepared organophilic clay was blending into the epoxy resin through an in-situ thermal ring-opening polymerization to prepare a series of PCN materials.

3.1. Characterization

The representative FTIR spectra of the organophilic clay, epoxy resin, and a series of PCN materials with various clay loadings were shown in Fig. 2. The spectroscopy confirmed
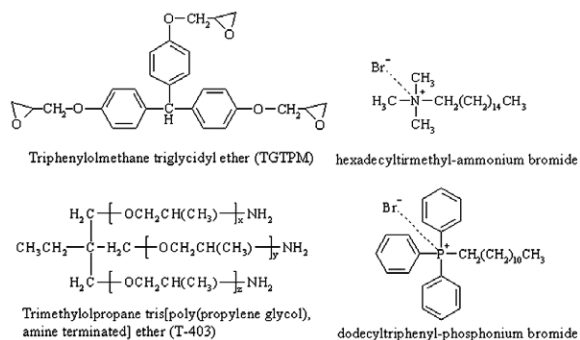

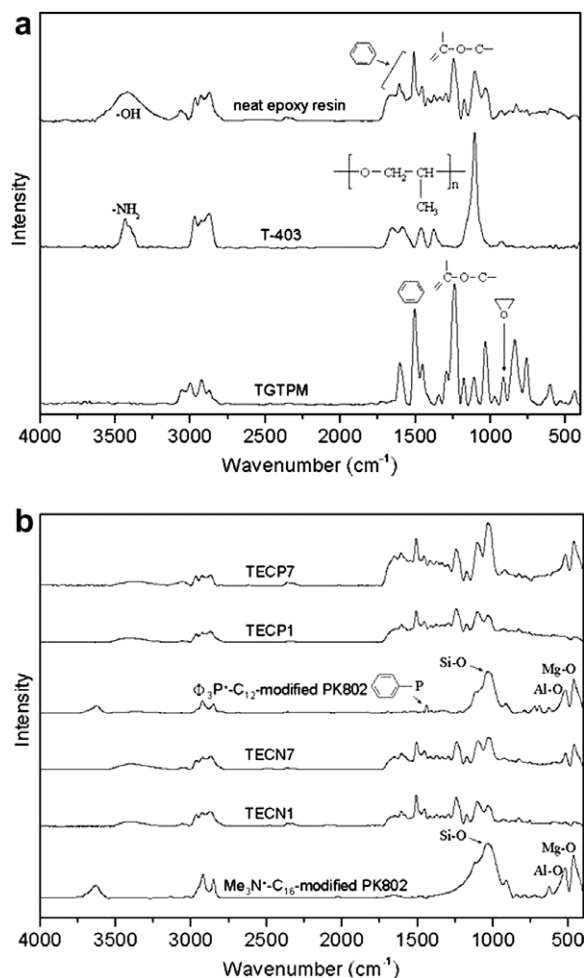Fig. 1. Chemical structures of Epoxy resin (TGTPM), hardener (T-403), and two kinds of intercalation agents.

Fig. 2. Representative FTIR spectra of (a) neat epoxy resin polymerization, (b) the both of modified Na+-MMT clay, and a series of PCN materials.

the completeness of the curing process (i.e., oxide-ring-opening polymerizations) between the epoxy ring of TGTPM and primary amine group of hardener T-403, as indicated by the diminishness and enhancement of characteristic peaks appeared at 915 cm^{-1} (i.e., epoxy ring) and 3380 cm^{-1} (i.e., -OH), as shown in Fig. 2(a). Moreover, the epoxy monomer was further reacting with the secondary hydroxyl groups of the high-molecular weight epoxy resin to form an ether linking at 1233 cm^{-1} (C–O–C) [17,18]. The vibration bands of dodecyltriphenyl-phosphonium (Φ_3P^+-C_{12}) MMT clay, and hexadecyltirmethyl-ammonium (Me_3N^+-C_{16}) MMT clay were shown at 3600 cm^{-1} (free H_2O), 2926 cm^{-1}, 2852 cm^{-1} (CH_2), 1478 cm^{-1} (Me–N), 1455 cm^{-1} (Acyl–P), 1040 cm^{-1} (Si–O), 510 cm^{-1} (Al–O), and 460 cm^{-1} (Mg–O). When the loading of organophilic MMT clay was increased, the intensities of those peaks become stronger, as illustrated in the FTIR spectra of PCN materials (Fig. 2(b)).

3.2. Morphological characteristics

The wide-angle powder XRD was used to determine the d-spacing of organophilic clays in epoxy resin matrix. As

MACROMOLECULAR NANOTECHNOLOGY
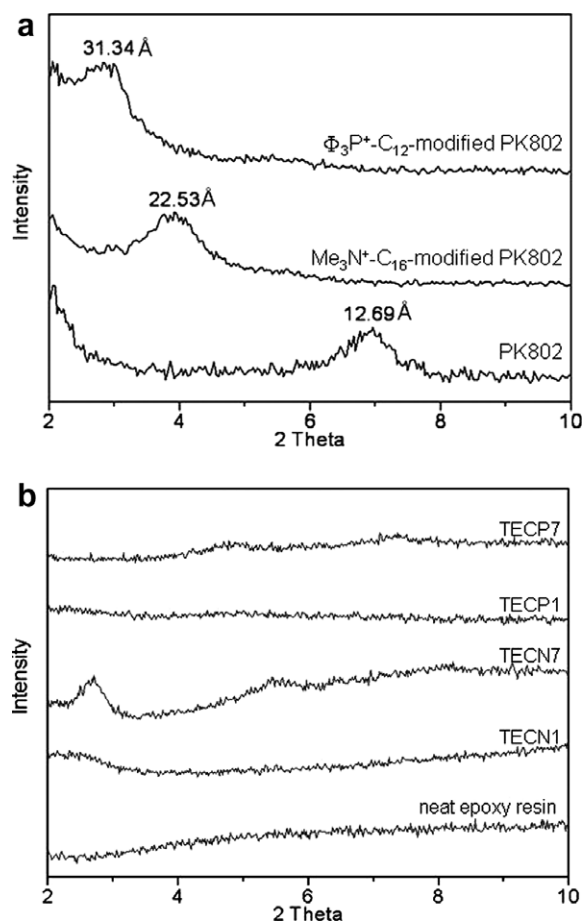
Fig. 3. Wide-angle powder X-ray diffraction patterns ranging between $2\theta = 2°$ and $2\theta = 10°$ of (a) the PK 802 and both two modified Na^+-MMT clay, and (b) neat epoxy resin and a series of PCN materials.

showed in Fig. 3(a) illustrated that the organophilic clay modified with Me_3N^+-C_{16} and Φ_3P^+-C_{12} had a d_{001} spacing of 22.53 Å ($2\theta = 3.92°$) and 31.34 Å ($2\theta = 2.82°$), respectively, and both were higher than the pristine Na^+-MMT clay with a d_{001} spacing of 12.69 Å ($2\theta = 6.96°$), which was calculated on the basis of Bragg's equation ($n\lambda = 2d \sin \theta$, $\lambda = 1.5418$ Å, Cu $K\alpha_1$). It indicated that the both cationic surfactants had been intercalated into the intragallery region of the clay layers through the cationic exchange reactions. It should be noted that the quaternary phosphonium salt-modified clay showed a larger d_{001}-spacing than that of quaternary ammonium salt-modified clay. After incorporation of organophilic clay into epoxy resin, we also found that the system containing quaternary phosphonium salt exhibited a better dispersion capability in polymer matrix, as shown in Fig. 3(b). For example, TECN7 revealed an obvious peak at $2\theta = 2.68°$ (d-spacing = 32.97 Å). However, for TECP7, there is a lack of any diffraction peak in $2\theta = 2-10°$ as opposed to the diffraction peak at $2\theta = 2.82°$ (d-spacing = 31.34 Å) for organophilic clay, indicating the possibility of having exfoliated silicate nanolayers of organophilic clay dispersed in an epoxy resin matrix.

A comparative study for the dispersion capability of organophilic clay modified with two different intercalation agents in the epoxy resin matrix can be further examined the TEM. As shown in Fig. 4, the TEM micrographs of TECP7 (Fig. 4(b)) exhibited a better dispersion capability of organophilic clay platelets as compared to that of TECN7 (Fig. 4(a)), which is consistent with the previous conclusions obtained from the powder XRD studies.

3.3. Anticorrosion properties of coatings

In this study, protective performance against corrosion of sample-coated CRS coupons in saline conditions was
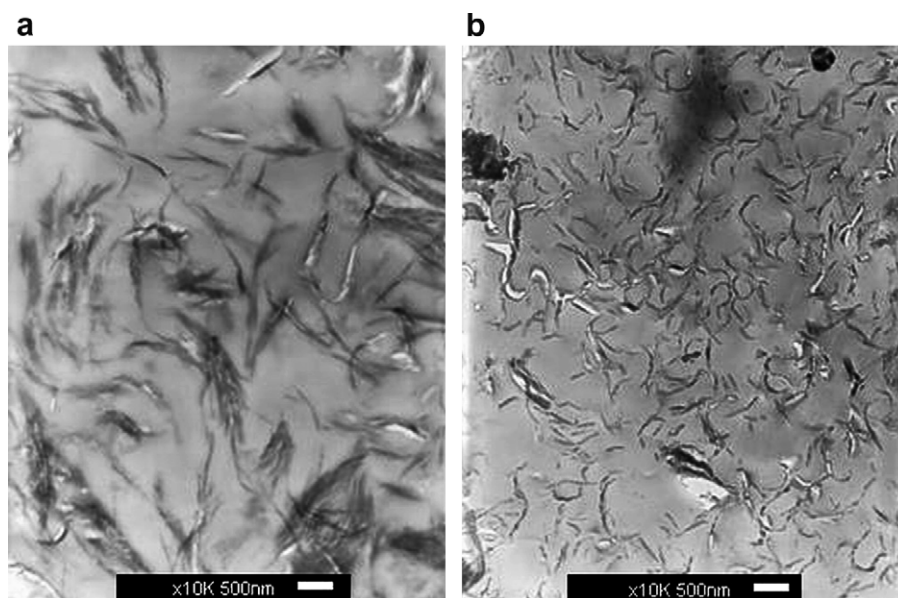
Fig. 4. Transmission electron microscopy of (a) TECN7 and (b) TECP7 at ×10 k magnification (scale bar = 500 nm).

MACROMOLECULAR NANOTECHNOLOGY

Table 1

Anticorrosive performance of epoxy resin-clay nanocomposite materials as measured form electrochemical corrosion measurement and barrier properties of the epoxy resin-clay nanocomposite materials

|	Feed composition (wt-%)		Electrochemical measurements					Barrier properties		
	Epoxy	Modified-MMT	E_{corr} (mV)	R_p (kΩ cm^2)	I_{corr} (μA/cm^2)	R_{corr} (MPY)	Thickness (mm)[c]	Permeability (g/m^2-h)[a]	Barrer (O$_2$)[b]	Thickness (mm)[c]
Bare	–	–	−722.4	4.99	2.6000	1.2133	–	–	–	–
Neat epoxy	100	0	−699.5	7.86	1.9840	0.9259	0.361	233.233	2.248	0.175
TECN1	99	1	−669.7	41.25	1.1698	0.5459	0.363	209.819	1.197	0.175
TECN3	97	3	−579.3	163.13	0.3844	0.1794	0.363	195.406	0.972	0.172
TECN5	95	5	−496.1	265.64	0.1634	0.0763	0.361	177.136	0.783	0.178
TECN7	93	7	−309.9	931.73	0.0269	0.0126	0.361	161.130	0.763	0.172
TECP1	99	1	−667.8	129.52	0.1776	0.0829	0.363	193.857	0.789	0.178
TECP3	97	3	−564.9	633.53	0.1571	0.0733	0.363	175.771	0.648	0.179
TECP5	95	5	−446.3	835.61	0.0599	0.0279	0.363	159.980	0.380	0.178
TECP7	93	7	−268.8	933.51	0.0214	0.0099	0.361	140.646	0.312	0.173

[a] As measured from VPA.
[b] As measured from GPA.
[c] As measured by a digimatic micrometer.

determined from a series of electrochemical parameter measurements such as corrosion potential (E_{corr}), polarization resistance (R_p), corrosion current (I_{corr}), and corrosion rate (R_{corr}), as listed in Table 1. The E_{corr}, R_p, I_{corr}, and R_{corr} for epoxy coating on CRS show better corrosion resistance compared to the uncoated CRS. Furthermore, the CRS coupon coated with PCN materials all show significantly higher values of E_{corr}, and R_p, and lower values of I_{corr}, and R_{corr} than the neat epoxy coating, as showed in Table 1. In addition, the TECP system exhibited higher corrosion potential than TECN system, for example, TECP7 exhibiting E_{corr} = −268.8 mV was superior to E_{corr} = −309.9 mV of TECN7. Such an E_{corr} value implied that the TECP-coated CRS coupon was more inert toward the electrochemical corrosion relative to the TECN-coated specimen [10]. Moreover, TECP1 presented the polarization resistance (R_p) of 129.52 kΩ cm^2 in 5 wt% NaCl, which was 3-fold of magnitude greater than the TECN1. The Tafel plots for (a) bare (naked cold-rolled steel, CRS), (b) pure epoxy resin, (c) TECN1, (d) TECP1, (e) TECN7, and (f) TECP7 were shown in Fig. 5. On the other hand, the corresponding corrosion current (I_{corr}) of TECP1 was *ca.* 0.1776 μA/cm^2, which cor-

responds to a corrosion rate (R_{corr}) of ca. 8.29×10^{-2} MPY, as shown in Table 1. Electrochemical parameters such as I_{corr} and R_{corr} values of TECP1 coated on CRS were found to decrease 93% as compared to 55% of TECN1.

Electrochemical impedance spectroscopy (EIS) was also used to examine the activity on the CRS surface treated by PCN coatings. Fig. 6 showed the Nyquist plots of the six measured samples (a) bare (naked cold-rolled steel, CRS), (b) pure epoxy resin, (c) TECN1, (d) TECP1, (e) TECN7, and (f) TECP7 in order. The corrosion of these samples in 5 wt% NaCl aqueous electrolyte for 30 min was followed by EIS. The charge-transfer resistances of those samples as determined by the intersection of the high-frequency end from the low-frequency end of the semicircle arc with the real axis were 1.03, 10.6, 90.9, 148, 490, and 600 kΩ cm^2, respectively [19]. The results clearly demonstrated that the PCN matrix with Φ_3P^+-C$_{12}$-modified clay had the greatest anticorrosive performance. EIS Bode plots (impedance vs. frequency) of samples (a–f) were shown in Fig. 7. In conclusion, the PCN coatings containing quaternary phosphonium salt-modified clay exhibited better corrosion protection performance on CRS coupons than that
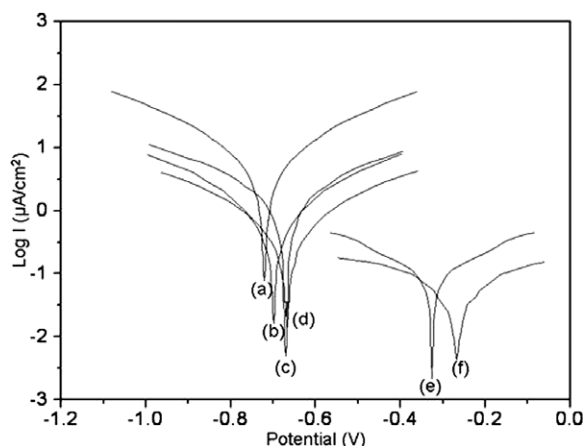
Fig. 5. The Tafel plots for (a) bare, (b) neat epoxy resin, (c) TECN1, (d) TECP1, (e) TECN7, and (f) TECP7 measured in 5 wt% NaCl aqueous solution.
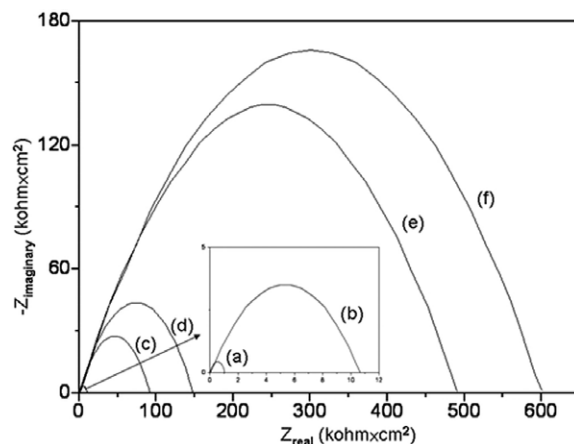
Fig. 6. Nyquist plots of ESI for (a) bare, (b) neat epoxy resin, (c) TECN1, (d) TECP1, (e) TECN7, and (f) TECP7 measured in 5 wt% NaCl aqueous solution.

with quaternary ammonium salt-modified clay based on the electrochemical corrosion parameter measurements such as Tafel plot, Bode plot, Nyquist plot, etc. The effective enhancement of anticorrosion effect for the TECP coatings system as compared to that of TECN system might have arisen from dispersing silicate nanolayers of clay in an epoxy resin matrix, leading to a much increase for the tortuosity of diffusion pathway of oxygen and water vapor. This can be further identified by the studied of O_2 and H_2O molecular barrier effect as discussed in the next section.

3.4. Barrier properties

As far as the results of anticorrosion properties were concerned, the favors penetration reduction by forcing diffusing molecules (i.e., a nematic phase) to make long detours round the platelets and changes in the local permeability [20]. The membranes used for the molecular permeability measurements were prepared to have a thickness of ca. ~0.175 mm. For the oxygen and water vapor permeability studies, meanwhile, we found that the incorporation of different organophilic clay into epoxy resin matrix results in a distinct reduction of barrier properties for epoxy resin-clay nanocomposite membranes, as listed in Fig. 8. Compared to that pure epoxy resin, freestanding films of TECP and TECN system at clay loading (e.g., 7 wt%) showed 86.1% and 66% reduction of oxygen permeability, respectively. Nevertheless, it should be further noted that an immense decrease in the amount of TECP7 was 92.58 g/m²-h extremely for the water vapor permeability studies, as illustrated in Table 1. For these, one factor should be considered, namely a geometric factor about the rigid phenyl group and long-chain alkyl group pendant in dodecyltriphenyl-phosphonium salt, could significantly result in an exfoliated clay structure [21].

3.5. Thermal and dynamic mechanical properties

The glass transition temperature (T_g) based on the DSC evaluations was found to increase form 83.63 °C of neat

Fig. 8. Permeability of water vapor (--) and gas permeability of oxygen (——) as a function with the organophilic MMT clay content in the epoxy resin-clay nanocomposite materials for (a) -●-, (c) −△− are TECP system and (b) -♦-, (d) −□− are TECN system.
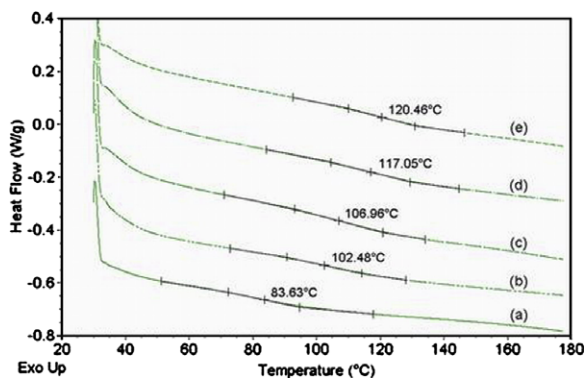
Fig. 9. Differential scanning calorimetry plots for (a) neat epoxy resin, (b) TECN1, (c) TECP1, (d) TECN7, and (e) TECP7.

polymer up to 120.46 °C of TECP7, as shown in Fig. 9 and Table 2. The effectively enhanced T_g of TECP7 may probably associated with the good dispersion of quaternary phosphonium salt-modified clay in polymer framework, which led to a large interfacial contact area between the inorganic clay platelets and organic epoxy resin matrix. Furthermore, the highly dense network of epoxy resin was also favored the interactions between the clay nano-layers by its homopolymerization within the clay galleries, and then polymer chains may be tied through the surface of the silicate by electrostatic interaction, thus increasing the surrounding entanglements [22,23].

Subsequently, the thermo-mechanical properties of composite materials were also investigated through the performing of DMA tests using a tension mode. Typically, two different moduli, i.e., elastic or storage modulus (E') and an imaginary (loss) modulus (E'') were identified in the curves of DMA thermograms. The ratio E'/E'', which typically reached a maximum point, was called tan delta (tan δ) and employed as glass transition temperature (T_g) of as-tested polymer. The curves in Fig. 10 illustrated the dependence of the storage modulus and the tan δ, respectively. The data also summarized the storage modulus
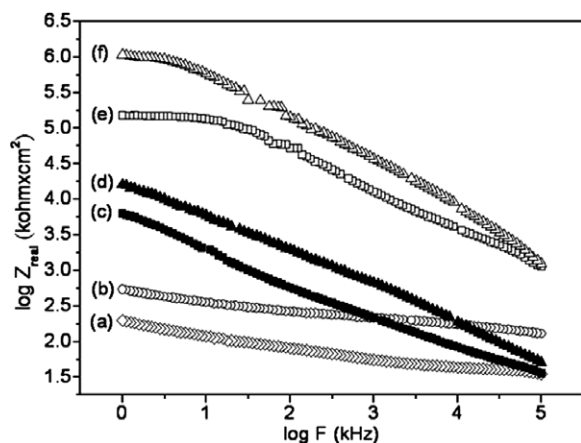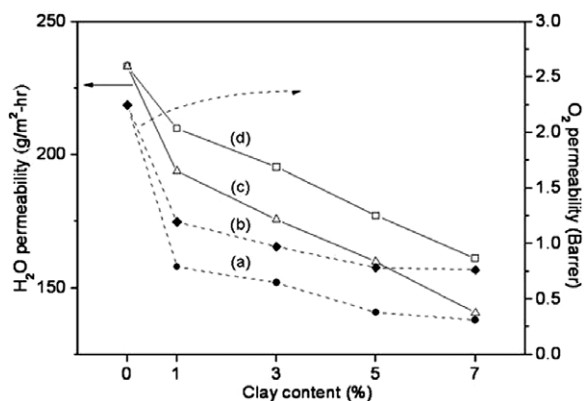

Fig. 7. Bode plots for (a) bare, (b) neat epoxy resin, (c) TECN1, (d) TECP1, (e) TECN7, and (f) TECP7 measured in 5 wt% NaCl aqueous solution.

MACROMOLECULAR NANOTECHNOLOGY

Table 2
Thermal properties of the epoxy resin-clay nanocomposite materials measured by TGA, DSC, DMA, and LOI

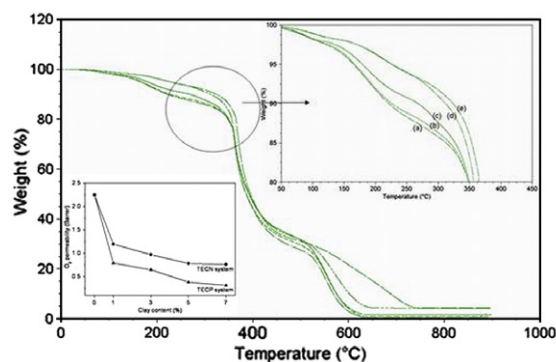|	T_d (°C)[a]	Char yield (wt-%)[b]	T_g (°C)[c]	LOI[d]	Storage modulus (E')[e] MPa		Tan Delta (°C)[e]
					35 °C	130 °C	
neat epoxy	346.2	0.048	83.63	19.0	2311	58.1	97.86
TECN1	352.7	0.729	102.48	20.5	2435	63.8	107.22
TECN3	353.9	2.167	105.59	22.0	f	f	f
TECN5	355.3	3.237	114.80	23.5	f	f	f
TECN7	357.2	4.678	117.05	24.5	3015	191.5	121.96
TECP1	353.6	0.798	106.96	23.0	2740	69.5	108.64
TECP3	355.1	2.325	108.16	24.5	f	f	f
TECP5	357.3	3.465	116.36	26.5	f	f	f
TECP7	359.5	4.830	120.46	27.5	3597	290.3	124.92

[a] As measured from TGA in air.
[b] As measured by TGA at 850 °C.
[c] As measured from DSC.
[d] ASTM D-2863. Sample size: 140 ± 5 mm × 52 ± 0.5 mm (type D), spending 3 min burning 8 cm.
[e] As measured by DMA.
[f] Not determined.
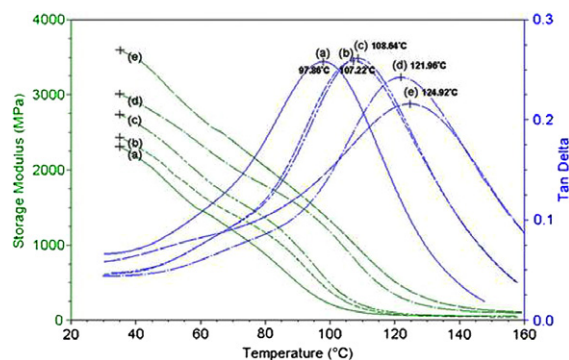
Fig. 10. Dynamic mechanical property of storage modulus (E′) and tangent δ plots for (a) neat epoxy resin, (b) TECN1, (c) TECP1, (d) TECN7, and (e) TECP7.

Fig. 11. Thermogravimetric analysis plots for (a) neat epoxy resin, (b) TECN1, (c) TECP1, (d) TECN7, and (e) TECP7.

values for the PCN materials at 35 °C (glassy region, below T_g) and at 130 °C (rubbery region, above T_g), along with the T_g values obtained from the maximum in tan δ, as shown in Table 2. The storage moduli of as-prepared materials in the glassy region, the superior dispersion of Φ_3P^+-C_{12}-modified clay in epoxy resin matrix led to an effective enhancement of mechanical strength. For example, the storage modulus was increased from the neat epoxy resin matrix of 2311 MPa up to TECP7 of 3597 MPa. Furthermore, the incorporation of organophilic clay in polymer matrix also exhibit significant improvements of mechanical strength of neat polymer matrix in the rubbery region shown in Table 2 for the evaluation of tan δ. For example, the T_g of the TECP7 was found to be higher than TECN7, which is probably due to the Brownian motion of network chains [18], and the results were consistent with our previous DSC studies.

3.6. Thermal stability and flame retardant performance

In the subsequent thermal property studies, enhancement of thermal stability, and thermal degradation behavior of polymer matrix via the formation of epoxy resin-clay

nanocomposite materials was determined by thermal decomposition temperatures (T_d) of as-prepared materials in TGA thermograms, as measured under an air atmosphere. In general, there appeared to be three stages of weight loss starting at ∼150 °C and ending at 800 °C, which might be correspondent to the degradation of intercalation agents (i.e., 150–250 °C) followed by the structural decomposition of uncrosslinked (i.e., 250–450 °C) and crosslinked (i.e., 500–650 °C) component of epoxy resin, as shown in Fig. 11 [24–26].

The flammability properties of the PCN materials were examined by measuring their corresponding LOI value. A significant increase in LOI value was observed as the organophilic clay was effectively dispersed in the epoxy resin matrix. For example, the LOI value of TECN7 and TECP7 was equal to 24.5 and 27.5, respectively, which was obviously higher than that of neat epoxy resin (i.e., LOI = 19). The higher LOI value of TECP7 as compared to that of TECN7, as shown in Table 2, may be probably due to the better organophilic clay dispersion of TECP7 in epoxy resin. In conclusion, the incorporation of organophilic clay into the epoxy resin matrix may exhibit a useful effect on leveling up the flame retardancy of the PCN materials.

4. Conclusion

In this article, a series of comparative studies for the effect of intercalating agent on the physical properties of the epoxy resin-clay based nanocomposite materials were performed. The quaternary alkylphosphonium and alkyl ammonium salt were both used as the intercalating agents separately for the preparation of organophilic clay through the cationic exchange reactions with Na^+-MMT clay, followed by blending the organophilic clay into the epoxy monomer and hardener through the thermal ring-opening polymerizations to give a series of PCN materials. The as-prepared materials were subsequently characterized by the sequential studies of FTIR spectroscopy, Wide-angle XRD diffraction and TEM. The morphological images for the organophilic clay was evidenced that the quaternary alkylphosphonium salt-modified clay (TECP system) exhibited a better dispersion capability in epoxy resin matrix than that of quaternary alkylammonium salt-modified clay (TECN system). The better dispersion of TECP system may lead to a larger interfacial contact area between the inorganic clay platelets and organic polymeric matrix, reflecting a remarkable enhancement of physical properties as compared to that of TECN system. For example, at same clay loading, all TECP system exhibited a better performance on corrosion protection, gas barrier, mechanical strength, thermal stability, and flame retardant properties as compared to that of TECN system based on the studies of a series of electrochemical corrosion parameter measurements, gas permeability analysis (GPA), dynamic mechanical analysis (DMA), differential scanning calorimetry (DSC), thermogravimetric analysis (TGA), and limiting oxygen index (LOI) test, respectively. Furthermore, effect of material composition on the physical properties of as-prepared materials was also investigated. The loading increase of organophilic clay in PCN materials usually accompanied with an increased of physical properties as mentioned in the previous sections.

References

[1] Lan T, Kaviratna PD, Pinnavaia TJ. Chem Mater 1994;6:573.
[2] Gilman JW, Jackson CL, Morgan AB, Harris Jr R, Manias E, Giannelis EP, et al. Chem Mater 2000;12:1866.
[3] Yao KJ, Song M, Hourston DJ, Luo DZ. Polymer 2002;43:1017.
[4] Tyan HL, Liu YC, Wei KH. Chem Mater 1999;11:1942.
[5] Yeh JM, Chen CL, Huang CC, Chang FC, Chen SC, Su PL, et al. J Appl Polym Sci 2006;99:1576.
[6] Li C, Wilkes GL. Chem Mater 2001;13:3663.
[7] Cho MS, Choi HJ, Ahn WS. Langmuir 2004;20:202.
[8] Yeh JM, Chen CL, Chen YC, Ma CY, Lee KR, Wei Y, et al. Polymer 2002;43:2729.
[9] Yeh JM, Yu MY, Liou SJ. J Appl Polym Sci 2003;89:3632.
[10] Yeh JM, Liou SJ, Lai CY, Wu PC. Chem Mater 2001;13(3):1131.
[11] Pluart LL, Duchet J, Sautereau H. Polymer 2005;46:12267.
[12] Akorna G, Ugi I. Angew Chem Int Ed Engl 1977;16:259.
[13] Nair CPR, Glouet G, Guilbert Y. Polym Degrad Stsb 1989;26:305.
[14] Yu YH, Jen CC, Huang HY, Wu PC, Huang CC, Yeh JM. J Appl Polym Sci 2004;91:3438.
[15] Yeh JM, Chin CP. J Appl Polym Sci 2003;88:1072.
[16] Deng J, Zhu S, Shi W. J Appl Polym Sci 2004;94:2065.
[17] Manfredi LB, Ginés MJL, Benítez GJ, Egli WA, Rissone H, Vázquez A. J Appl Polym Sci 2005;95:1448.
[18] Ochi M, Takahashi R. J Appl Polym Sci: Part B: Polymer Physics 2001;39:1071.
[19] Li P, Tan TC, Lee JY. Synth Met 1997;88:237.
[20] Fredrickson GH, Bicerano JJ. Chem Phys 1999;110:2181.
[21] Korman X. Polymer 2002;54:1403.
[22] Nigam V, Setua DK, Mathur GN, Kar KK. J Appl Polym Sci 2004;93:2201.
[23] Jeng RJ, Lo GS, Chen CP, Liu YL, Hsiue GH, Su WC. Polym Adv Technol 2003;14:147.
[24] Hasegawa K, Fukuda A, Tonogi SJ. Appl Polym Sci 1989;37:3423.
[25] Lji M, Kiuchi Y, Soyama M. Polym Adv Technol 2003;14:638.
[26] Musto P, Ragosta G, Russo P, Mascia L. Macromol Chem Phys 2001;202:3445.

MACROMOLECULAR NANOTECHNOLOGY